Revision 1

Beshtauite, $(NH_4)_2(UO_2)(SO_4)_2 \cdot 2H_2O$, a new mineral from Mount Beshtau, Northern Caucasus, Russia

Igor V. Pekov[1]*, Sergey V. Krivovichev[2], Vasiliy O. Yapaskurt[1], Nikita V. Chukanov[3] and Dmitriy I. Belakovskiy[4]

[1] Faculty of Geology, Moscow State University, Vorobievy Gory, 119991 Moscow, Russia

[2] Faculty of Geology, St Petersburg State University, University Embankment 7/9, 199034 St Petersburg, Russia

[3] Institute of Problems of Chemical Physics, Russian Academy of Sciences, 142432 Chernogolovka, Moscow Oblast, Russia

[4] Fersman Mineralogical Museum of the Russian Academy of Sciences, Leninsky Prospekt 18-2, 119071 Moscow, Russia

* Corresponding author. E-mail: igorpekov@mail.ru

Running title: Beshtauite, a new mineral

ABSTRACT

A new mineral beshtauite, $(NH_4)_2(UO_2)(SO_4)_2 \cdot 2H_2O$, was found in the oxidation zone of the Beshtau uranium deposit, Mount Beshtau, Stavropol region, Northern Caucasus, Russia, and named after the locality. It is associated with rozenite, gypsum, lermontovite and older marcasite, pyrite, halloysite and opal. Beshtauite occurs as well-shaped short-prismatic crystals up to 0.1 x

0.15 x 0.2 mm, their clusters and crusts up to 0.5 mm across growing on marcasite. Beshtauite is transparent, light-green. The luster is vitreous. The mineral fluoresces strongly yellow-green under both short- and long-wave UV irradiation. It is brittle. The Mohs hardness is *ca*. 2. Cleavage was not observed. $D_{calc.}$ is 3.046 g cm^{-3}. Beshtauite is optically biaxial (+), α = 1.566(3), β = 1.566(3), γ = 1.592(3), 2V (meas.) < 10º. The chemical composition (wt%, electron microprobe data, H_2O by difference) is: $(NH_4)_2O$ 10.33, UO_3 53.21, SO_3 29.40, H_2O (calc.) 7.06, total 100.00. Content of $(NH_4)_2O$ was calculated from measured nitrogen content: 5.56 wt% N. The empirical formula, calculated on the basis of 12 O *apfu*, is: $(NH_4)_{2.12}U_{0.99}S_{1.96}O_{9.91}(H_2O)_{2.09}$. Beshtauite is monoclinic, $P2_1/c$, a = 7.7360(8), b = 7.3712(5), c = 20.856(2) Å, β = 102.123(8)º, V = 1162.76(19) Å^3, Z = 4 (from single-crystal X-ray diffraction data). The strongest reflections of the X-ray powder pattern [d,Å-I(hkl)] are: 6.86-100(011, 10-2); 5.997-19(012); 5.558-15(102); 5.307-36(11-1, 110); 5.005-35(013, 11-2); 3.410-38(114, 20-4, 10-6), 3.081-24(016), 2.881-20(106, 123). The crystal structure was solved by direct methods and refined on the basis of 2677 independent reflections with $I > 4\sigma(I)$ to R_1 = 0.093. The structure is based upon $[UO_2(SO_4)_2(H_2O)]^{2-}$ layers consisting of corner-sharing $UO_6(H_2O)$ pentagonal bipyramids and SO_4 tetrahedra. The layers are coplanar to (-102) and are linked via hydrogen bonding that involve interlayer NH_4^+ ions and H_2O molecules. Beshtauite is important indicator mineral: its presence can be considered as an evidence of transportation of U^{6+} in nature in forms of mobile complexes of uranyl cation with ammonia or polyamines.

Keywords: beshtauite; new mineral; ammonium uranyl sulfate; crystal structure; oxidation zone; Beshtau; Northern Caucasus.

INTRODUCTION

Uranium sulfates are important secondary minerals formed in the oxidation zones of uranium deposits (Čejka and Urbanec 1990; Finch and Murakami 1999; Krivovichev and Plášil 2013). Recent studies led to considerable advances in knowledge and understanding of formation and crystal chemistry of uranium sulfates, both with tetra- and hexavalent uranium ions (Plášil et al. 2010, 2011a, b, c, 2012a, b, c, 2013a, b). As a rule, natural uranium sulfates crystallize from highly acidic solutions resulted from acid-mine drainage due to the oxidation of primary sulfide minerals (Chernikov 1981). In this paper we report on the occurrence, chemistry, structure and properties of a new mineral species, the first natural ammonium uranyl sulfate that was discovered during the studies of secondary uranium mineralization of the deposits in Northern Caucasus. It was found in several samples from the old collections from the Beshtau uranium deposit (also known under names Beshtaugorskoe or Lermontovskoe) at Mount Beshtau (44°05'53"N 43°01'20"E) located between the cities of Pyatigorsk, Lermontov and Zheleznovodsk in the Stavropol region, Russia. The new mineral was named beshtauite (Cyrillic: бештауит) after the type locality. Its holotype specimen was extracted by us from the material collected in 1950s by well-known Russian mineralogist, specialist in the uranium deposits Vyacheslav Gavrilovich Melkov (1911–1991), who provided the samples to the Geological Museum of All-Russian Scientific Research Institute of Mineral Resources (VIMS), Moscow.

The new mineral and its name have been approved by the IMA CNMNC, No. 2012–051. The type specimen of beshtauite is deposited in the systematic collection of the Fersman Mineralogical Museum of the Russian Academy of Sciences, Moscow, under the catalogue number 93775.

OCCURRENCE AND GENERAL APPEARANCE

The Beshtau deposit was in operation for uranium underground mining in the period from 1950 to 1974. The deposit consists of numerous hydrothermal veins containing uraninite and

coffinite in porphyry granites. The upper part of the deposit is intensively oxidized and contains diverse secondary uranium mineralization. In particular, lermontovite, $U^{4+}(PO_4)\cdot H_2O$, was first discovered here (Melkov, 1958; Melkov et al. 1983).

Beshtauite was found at the Gremuchka ore zone in the eastern part of the Beshtau deposit. The specimens with the mineral were collected from the partially oxidized marcasite vein containing subordinate pyrite, halloysite, opal, and uraninite and cross-cutting porphyry granite in the fault zone. The supergene minerals are lermontovite, beshtauite, rozenite and gypsum.

Beshtauite occurs as well-shaped short-prismatic crystals up to 0.1 x 0.15 x 0.2 mm in size (Figure 1a), clusters of crystals (Figure 1b) and crystal crusts up to 0.5 mm thick on the surface of marcasite crusts (Figure 1c). Aggregates (up to 0.5 mm) of anhedral grains of the new mineral on marcasite were also observed. Optical examination shows that beshtauite crystals looking perfectly under the microscope (Figure 1), however, typically have a mosaic character, which significantly hampered their single-crystal X-ray diffraction studies.

PHYSICAL PROPERTIES AND OPTICAL DATA

Beshtauite is transparent, light-green. Crystals typically look dark green due to the abundant micro-inclusions of marcasite. The streak is white. The luster is vitreous. The mineral fluoresces strongly yellow-green under both short- and long-wave ultraviolet irradiation. Beshtauite is brittle. The Mohs hardness is *ca*. 2. Cleavage and parting were not observed, the fracture is uneven. Density could not be measured because of the absence of relatively large crystals without marcasite inclusions; the calculated density is 3.046 g cm^{-3}. The mineral is radioactive.

Beshtauite is optically biaxial positive, $\alpha = 1.566(3)$, $\beta = 1.566(3)$, $\gamma = 1.592(3)$ (589 nm). Measured 2V is low, $< 10^{o}$; 2V (calc.) = 0^{o}. Dispersion of optical axes is not observed. Under the microscope, the mineral is colorless, nonpleochroic.

INFRARED SPECTROSCOPY

Beshtauite powder was mixed with anhydrous KBr, pelletized, and analyzed (16 scans) using an ALPHA FTIR spectrometer (Bruker Optics) at the resolution of 4 cm^{-1}. IR spectrum of an analogous pellet of pure KBr was used as a reference.

The IR spectrum of beshtauite (Figure 2) is unique for minerals but very close to that of synthetic $(NH_4)_2(UO_2)(SO_4)_2 \cdot 2H_2O$ reported by Niinisto et al. (1978).

Absorption bands in the IR spectrum of beshtauite and their assignments [cm^{-1}; s – strong band, w – weak band; for the assignment of the bands of uranyl ions see Čejka (1999)] are: 3550 (O–H-stretching vibrations of H_2O molecules), 3233s (N–H-stretching vibrations of NH_4^+ groups probably overlapped with O–H-stretching vibrations of H_2O molecules), 3105 (N–H-stretching vibrations of NH_4^+ cations), 1603 (H–O–H bending vibrations of H_2O molecules), 1438 (H–N–H bending vibrations of NH_4^+ cations), 1175, 1143, 1117s, 1071 (asymmetric S–O stretching vibrations of SO_4^{2-} anions), 1033s, 1003s (symmetric S–O stretching vibrations of SO_4^{2-} anions), 928 (antisymmetric U–O stretching vibrations of UO_2^{2+} cations), 840w, 806w (symmetric U–O stretching vibrations of UO_2^{2+} cations), 642, 617, 598, 591 (O–S–O bending vibrations), 421 (lattice mode possibly involving librational vibrations of UO_2^{2+}, SO_4^{2-} and H_2O). The splitting of the non-degenerate band of symmetric S–O stretching vibrations of SO_4^{2-} anions indicates the presence of two non-equivalent SO_4 tetrahedra. High intensities of these bands, as well as strong splitting of the bands of degenerate asymmetric S–O stretching vibrations of SO_4^{2-} anions reflect a rather strong distortion of SO_4 tetrahedra (see below).

CHEMICAL DATA

Chemical data for beshtauite were obtained using a Jeol JSM-6480LV scanning electron microscope equipped with an INCA-Wave 500 wavelength-dispersive spectrometer, with an acceleration voltage of 15 kV and a beam current of 20 nA. The electron beam was rastered to

the area of 10 x 10 μm^2 to minimize the damage of unstable sample. The following standards were used: $(NH_4)_2SO_4$ (N), UO_3 (U) and $BaSO_4$ (S). Content of H belonging to NH_4^+ cations and H_2O molecules was not measured because of scarcity of pure material, but the presence of these constituents was clearly confirmed by IR spectroscopy.

The average (7 analyses) chemical composition of beshtauite (wt%, ranges are in parentheses) is: $(NH_4)_2O$ 10.33 (8.9–11.4), UO_3 53.21 (52.4–54.1), SO_3 29.40 (28.8–30.2), H_2O (calc.) 7.06, total 100.00. Content of $(NH_4)_2O$ was calculated from measured nitrogen content: mean 5.56, range 4.8 – 6.1 wt% N. Content of H_2O was calculated by analytical total difference. Contents of other elements with atomic numbers higher than 6 are below detection limits.

The empirical formula of beshtauite, calculated on the basis of 12 O *apfu*, is $(NH_4)_{2.12}U_{0.99}S_{1.96}O_{9.91}(H_2O)_{2.09}$. The idealized formula is $(NH_4)_2(UO_2)(SO_4)_2{\cdot}2H_2O$, which requires $(NH_4)_2O$ 9.75, UO_3 53.53, SO_3 29.97, H_2O 6.75, total 100.00 wt%.

Beshtauite slowly dissolves in H_2O at room temperature.

X-RAY CRYSTALLOGRAPHY

X-ray powder diffraction data of beshtauite were collected using a STOE IPDS II diffractometer equipped with Image Plate area detector, using the Gandolfi method (Mo*K*α-radiation; detector-to-sample distance: 200 mm). Data are given in Table 1. Monoclinic unit cell parameters refined using least-squares technique from the powder data are: a = 7.74(1), b = 7.379(7), c = 20.85(3) Å, β = 102.0(1)º, V = 1164(4) Å^3.

Single-crystal X-ray studies of beshtauite were carried out using the same diffractometer. Unit-cell data and the experimental details are given in Table 2.

CRYSTAL STRUCTURE: DETERMINATION, DESCRIPTION AND DISCUSSION

Experimental

The selected crystal of beshtauite was mounted on a STOE IPDS II X-ray diffractometer equipped with Image Plate area detector and operated at 50 kV and 40 mA. More than a hemisphere of three-dimensional data was collected using monochromatic MoK_α X-radiation, with frame widths of 2° in ω, and with a 5 min count for each frame. The unit-cell parameters (Table 2) were refined using least-squares techniques. The intensity data were integrated and corrected for Lorentz, polarization, and background effects using the STOE X-Red program. An analytical absorption correction was made on the basis of experimentally determined crystal shape by means of the X-Shape 2.07 program (Stoe 2005).

The SHELX program package (Sheldrick 2008) was used for the refinement of the crystal structure. The coordinates published by Niinisto et al. (1978) for synthetic $(NH_4)_2(UO_2)(SO_4)_2{\cdot}2H_2O$ were used. The structure was refined in the monoclinic space group $P2_1/c$ by direct methods to an R_1 value of 0.093, calculated for the 2677 unique observed ($|F_o| \geq 4\sigma_F$) reflections. The poor quality of the beshtauite crystals was the reason for rather value of high crystallographic agreement index and did not allow determination of positions of H atoms. It was also the reason for the appearance of rather high residual electron density peaks in the difference Fourier maps, located close to the positions of the U atoms. The final refinement included anisotropic displacement parameters for all non-H atoms and a refinable weighting scheme. Final atom coordinates and displacement parameters of the atoms are given in Table 3, selected interatomic distances are in Table 4.

Results and Discussion

Beshtauite is a natural analogue of synthetic $(NH_4)_2(UO_2)(SO_4)_2{\cdot}2H_2O$ reported by Niinisto et al. (1978). Its crystal structure contains one symmetrically independent U site, which is linked to two O atoms to form a linear uranyl cation, $(UO_2)^{2+}$, with the U=O bond lengths of 1.776-1.791 Å. The uranyl cation is equatorially coordinated by four O atoms and one H_2O molecule to form the $UO_6(H_2O)$ pentagonal bipyramid. The uranium-oxygen bond lengths are in

182 good agreement with the average values reported by Burns et al. (1997). The bond-valence sum
183 incident upon the U site is 5.93 valence units (v.u.) as calculated using bond-valence parameters
184 provided by Burns et al. (1997).

185 There are two tetrahedrally coordinated S^{6+} cations in the structure that form $(SO_4)^{2-}$
186 tetrahedra with the average <S-O> bond lengths of 1.468 and 1.465 Å, respectively. These
187 values are in general agreement with the average <S-O> distance in sulfates (1.475 Å;
188 Hawthorne et al. 2000) and in uranyl sulfates in particular (1.473(2) Å; Krivovichev 2013). The
189 bond-valence sums for the S1 and S2 sites calculated using bond-valence parameters taken from
190 Brese and O'Keeffe (1991) are equal to 6.10 and 6.18 v.u., respectively.

191 The structure contains two symmetrically independent NH_4^+ cations that are involved in
192 four $NH_4\cdots O$ hydrogen bonds (N-O distances in the range of 2.90-3.11 Å) each with the adjacent
193 O atoms.

194 The crystal structure is based upon the $[UO_2(SO_4)_2(H_2O)]^{2-}$ layers consisting of corner-
195 sharing $UO_6(H_2O)$ pentagonal bipyramids and SO_4 tetrahedra (Figure 3). Each SO_4 tetrahedron
196 shares two of its O atoms with adjacent uranium polyhedra. As a consequence, the S-O_{br} bond
197 lengths for the bridging O_{br} atoms are slightly longer (1.478-1.502 Å) than the S-O_t bonds to the
198 terminal O_t atoms (1.419-1.465 Å). These values are in agreement with the average <S-O_{br}> and
199 <S-O_t> bond lengths of 1.483(1) and 1.455(1) Å found for the structures of uranyl sulfates
200 (Krivovichev 2013). The U-O_{br}-S bond angles in beshtauite are 141.7(7), 136.5(6), 140.4(8), and
201 143.4(8)^o for the O3, O4, O7, and O8 atoms, respectively, in excellent agreement with the
202 average value of 142.3(6)^o (Krivovichev 2013 ; Krivovichev and Plášil 2013).

203 The $[UO_2(SO_4)_2(H_2O)]^{2-}$ layers are coplanar to (-102) and are linked via hydrogen
204 bonding that involve interlayer NH_4^+ ions and H_2O molecules. The topology of the
205 interpolyhedral linkage of the layers is of the goldichite type, which is common in many
206 inorganic oxysalts and, in particular, in uranyl oxysalts (Graeber and Rosenzweig 1971;
207 Krivovichev 2008a, b). The topology is related to that observed for the $[UO_2(SO_4)_2(H_2O)]^{2-}$

208 layers in leydetite, $Fe(UO_2)(SO_4)_2(H_2O)_{11}$ (Plášil et al. 2013b). The $[UO_2(SO_4)_2(H_2O)]^{2-}$ layers in
209 both beshtauite and leydetite are based upon corner-sharing $UO_6(H_2O)$ pentagonal bipyramids
210 and SO_4 tetrahedra. However, the layers should be considered as different topological isomers
211 with the layer in beshtauite having the goldichite topology and the layer in leydetite possessing
212 rhomboclase topology (Krivovichev 2008a, b).
213

214 ## IMPLICATIONS

215 The discovery of beshtauite further extends our knowledge about the mineralogy and
216 crystal chemistry of uranium in oxidation zones of uranium mineral deposits. It is very likely that
217 beshtauite, because of its solubility in water, is an ephemeral species that was formed from
218 highly acidic aqueous solutions responsible for the transportation of uranium from primary ores
219 to the areas of secondary crystallization. The presence of beshtauite can be considered as an
220 evidence of transportation of U^{6+} in nature in forms of mobile complexes of uranyl cation with
221 ammonia or polyamines that is studied in synthetic systems (Zanello et al. 1978). Therefore
222 beshtauite is important mineral that detects structure and energetics of uranium complexes that
223 form at the initial stages of uranium dissolution in acidic waters generated by oxidation of sulfide
224 minerals.
225

226 ## ACKNOWLEDGEMENTS

227 We thank Nina V. Skorobogatova and Nadezhda E. Korosteleva for the providing of
228 samples for studies, referee Jakub Plášil for valuable comments and Beda Hofmann for editorial
229 work. This study was supported by the Russian Foundation for Basic Research, grant no. 11-05-
230 00397-a and St.Petersburg State University (internal grant 3.38.136.2014). Technical support by
231 the SPbSU X-Ray Diffraction Resource Center is gratefully acknowledged.
232
233

REFERENCES

Brese, N.E. and O'Keeffe, M. (1991) Bond-valence parameters for solids. Acta Crystallographica, **B47**, 192-197.

Burns, P.C., Ewing, R.C. and Hawthorne, F.C. (1997) The crystal chemistry of hexavalent uranium: polyhedron geometries, bond-valence parameters, and polymerization of polyhedra. Canadian Mineralogist, **35**, 1551-1570.

Čejka, J. (1999) Infrared spectroscopy and thermal analysis of the uranyl minerals. Reviews in Mineralogy and Geochemistry, **38**, 521-622.

Čejka, J. and Urbanec, Z. (1990) Secondary Uranium Minerals. Academia, Czechoslovak Academy of Sciences, Prague, Czech Republic.

Chernikov, A.A. (1981) Behaviour of Uranium in the Hypergene Zone. Nedra, Moscow (in Russian).

Finch, R.J. and Murakami, T. (1999) Systematics and paragenesis of uranium minerals. In: Burns, P.C. and Finch, R., Eds. Uranium: Mineralogy, Geochemistry and the Environment. Reviews in Mineralogy and Geochemistry, **38**, 91-180.

Graeber, E.J. and Rosenzweig, A. (1971) The crystal structures of yavapaiite, $KFe(SO_4)_2$, and goldichite, $KFe(SO_4)_2(H_2O)_4$. American Mineralogist, **56**, 1917-1933.

Krivovichev, S.V. (2008a) Crystal chemistry of selenates with mineral-like structures: V. crystal structures of $(H_3O)_2[(UO_2)(SeO_4)_2(H_2O)](H_2O)_2$ and $(H_3O)_2[(UO_2)(SeO_4)_2(H_2O)](H_2O)$, new compounds with rhomboclase and goldichite topology. Geology of Ore Deposits, **50**, 789-794 (translated from: Zapiski Rossiiskogo Mineralogicheskogo Obshchestva, 2008, **134(1)**, 54-61, in Russian).

Krivovichev, S.V. (2008b) Structural Crystallography of Inorganic Oxysalts. Oxford University Press, Oxford.

Krivovichev, S.V. (2013) Crystal chemistry of uranium oxides and minerals. In: Reedijk, J. and Poeppelmeier, K., Eds. Comprehensive Inorganic Chemistry II, Vol 2, 611-640. Elsevier, Oxford.

Krivovichev, S.V. and Plášil, J. (2013) Mineralogy and crystallography of uranium. In: Burns PC, Sigmon GE (eds) Uranium: Cradle to Grave. Mineralogical Association of Canada Short Course Series, **43**, 15-120.

Melkov, V.G. (1958) Additional explanations on discovery of new uranium minerals in the USSR. Proceedings of United Nations International Conference on the Peaceful Uses of Atomic Energy (8-20 August 1955), **6**, 966. Gosgeoltekhizdat, Moscow (in Russian).

Melkov, V.G., Belova, L.N., Gorshkov, A.I., Ivanova, O.A., Sivtsov, A.I. and Boronikhin, V.A. (1983) New data on lermontovite. Mineralogicheskiy Zhurnal, **5(1)**, 82-87 (in Russian).

Niinisto, L., Toivonen, J. and Valkonen, J. (1978). Uranyl(VI) compounds. I. The crystal structure of ammonium uranyl sulfate dihydrate, $(NH_4)_2UO_2(SO_4)_2{\cdot}2H_2O$. Acta Chemica Scandinavica, **A32**, 647-651.

Plášil, J., Buixaderas, E., Čejka, J., Sejkora, J., Jehlička, J. and Novák, M. (2010) Raman spectroscopic study of the uranyl sulphate mineral zippeite: low wavenumber and U–O stretching regions. Analitical and Bioanalitical Chemistry, **397**, 2703–2715.

Plášil, J., Mills, S.J., Fejfarová, K., Dušek, M., Novák, M., Škoda, R., Čejka, J. and Sejkora, J. (2011a) The crystal structure of natural zippeite $K_{1.85}H^+_{0.15}[(UO_2)_4O_2(SO_4)_2(OH)_2](H_2O)_4$, from Jáchymov, Czech Republic. Canadian Mineralogist, **49**, 1089-1103.

Plášil, J., Dušek, M., Novák, M., Čejka, J., Císařová, I., and Škoda, R. (2011b) Sejkoraite-(Y), a new member of the zippeite group containing trivalent cations from Jáchymov (St. Joachimsthal), Czech Republic: description and crystal structure refinement. American Mineralogist, **96**, 983-991.

Plášil, J., Fejfarová, K., Novák, M., Dušek, M., Škoda, R., Hloušek, J., Čejka, M., Majzlan, J., Sejkora, J., Machovič, V. and Talla, D. (2011c) Běhounekite, $U(SO_4)_2(H_2O)_4$, from

Jáchymov (St. Joachimsthal), Czech Republic: the first natural U^{4+} sulphate. Mineralogical Magazine, **75**, 2739-2753.

Plášil, J., Hloušek, J., Veselovský, F., Fejfarová, K., Dušek, M., Škoda, R., Novák, M., Čejka, J., Sejkora, J. and Ondruš, P. (2012a) Adolfpateraite, $K(UO_2)(SO_4)(OH)(H_2O)$, a new uranyl sulphate mineral from Jáchymov, Czech Republic. American Mineralogist, **97**, 447-454.

Plášil, J., Fejfarová, K., Wallwork, K.S., Dušek, M., Škoda, R., Sejkora, J., Čejka, J., Veselovský, F., Hloušek, J., Meisser, N. and Brugger, J. (2012b) Crystal structure of pseudojohannite, with a revised formula, $Cu_3(OH)_2[(UO_2)_4O_4(SO_4)_2](H_2O)_{12}$. American Mineralogist, **97**, 1796-1803.

Plášil, J., Hauser, J., Petříček, V., Meisser, N., Mills, S.J., Škoda, R., Fejfarová, K., Čejka, J., Sejkora, J., Hloušek, J., Johannet, J.M., Machovič, V. and Lapčák, L. (2012c) Crystal structure and formula revision of deliensite, $Fe[(UO_2)_2(SO_4)_2(OH)_2](H_2O)_7$. Mineralogical Magazine, **76**, 2837–2860.

Plášil, J., Fejfarová, K., Škoda, R., Dušek, M., Čejka, J. and Marty, J. (2013a) The crystal structure of magnesiozippeite, $Mg[(UO_2)_2O_2(SO_4)](H_2O)_{3.5}$, from East Saddle Mine, San Juan County, Utah (U.S.A.). Mineralogy and Petrology, **107**, 211-219.

Plášil, J., Kasatkin, A.V., Škoda, R., Novak, M., Kallistova, A., Dušek, M., Skála, R., Fejfarová, K., Čejka, J., Meisser, N., Goethals, H., Machovič, V. and Lapčák, L. (2013b) Leydetite, $Fe(UO_2)(SO_4)_2(H_2O)_{11}$, a new uranyl sulfate mineral from Mas d'Alary, Lodève, France. Mineralogical Magazine, **77**, 429-441.

Sheldrick, G.M. (2008) A short history of *SHELX*. Acta Crystallographica, **A64**, 112-122.

Stoe, GmbH (2005) X-Shape, Version 2.07.

Zanello, P., Cinquantini, A., Seeber, R. and Pieri, G. (1978) Polarographic investigations on uranyl(VI) complexes in dimethylsulfoxide. IV. Ammonia and polyamines. Inorganica Chimica Acta, **29**, 171-176.

310 Table 1. X-ray powder diffraction data for beshtauite
311

I_{obs}	d_{obs}, Å	I_{calc}	d_{calc}, Å*	*h k l*
100	6.86	21, 100	6.932, 6.796	011, 10-2
19	5.997	12	5.974	012
15	5.558	13	5.543	102
36	5.307	9, 9	5.303, 5.279	11-1, 110
35	5.005	6, 5	4.997, 4.996	013, 11-2
14	4.507	8	4.501	11-3
11	3.960	6	3.969	11-4
10	3.797	11	3.782	200
8	3.617	4	3.627	021
38	3.410	9, 4, 3, 8, 3, 10	3.425, 3.424, 3.399, 3.398, 3.389, 3.376	114, 21-1, 006, 20-4, 21-2, 10-6
17	3.243	4, 1, 5	3.240, 3.225, 3.224	023, 211, 121
24	3.081	1, 5, 3, 2	3.092, 3.086, 3.086, 3.069	12-3, 016, 21-4, 122
10	3.033	5, 3	3.031, 3.020	212, 115
6	2.999	2	2.987	024
20	2.881	11, 5, 2	2.882, 2.876, 2.872	106, 123, 21-5
6	2.786	1, 6	2.814, 2.772	213, 204
9	2.730	3, 1	2.734, 2.725	025, 11-7
2	2.655	1	2.652	21-6
6	2.577	4, 2	2.577, 2.570	30-2, 221
6	2.459	3	2.463	125
10	2.395	1, 1, 3, 1	2.406, 2.405, 2.389, 2.386	117, 31-3, 032, 215
11	2.345	3, 1, 1, 1, 2, 2	3.355, 2.347, 2.347, 2.339, 2.337, 2.336	20-8, 223, 31-4, 13-1, 130, 302
7	2.284	2	2.285	027
6	2.267	3	2.265	30-6
4	2.202	1	2.195	216
7	2.176	2, 1	2.179, 2.174	13-4, 118
3	2.117	2	2.116	22-7
14	2.077	2, 2, 3, 1	2.082, 2.081, 2.074, 2.074	1.0.-10, 225, 134, 23-1
4	1.996	1, 2	1.999, 1.992	32-5, 036
5	1.985	1	1.980	119
4	1.936	3, 1	1.934, 1.933	208, 40-2
4	1.904	2, 1	1.908, 1.901	40-4, 315
4	1.853	1, 1, 2	1.859, 1.858, 1.848	23-6, 41-1, 306
5	1.780	1, 1, 1	1.781, 1.779, 1.779	13-8, 14-2, 3.0.-10
5	1.745	1, 1, 1	1.749, 1.744, 1.742	142, 33-4, 412
4	1.685	1, 1	1.685, 1.679	32-9, 236
4	1.660	1, 1	1.663, 1.657	404, 240
3	1.633	1	1.634	2.2.-11
3	1.621	1	1.618	14-6
4	1.593	1, 1, 1	1.593, 1.591, 1.591	334, 42-7, 318
2	1.538	1	1.540	2.3.-10
2	1.506	1	1.504	50-6
3	1.443	1, 1	1.444, 1.441	3.0.10, 2.0.12
2	1.413	1	1.415	52-1

312 *Calculated for unit cell parameters obtained from single-crystal data.
313

Table 2. Crystallographic data and refinement parameters for beshtauite

Crystal data	
Temperature	293 K
Radiation, wavelength	MoK_α, 0.71073 Å
Crystal system	monoclinic
Space group	$P2_1/c$
Unit-cell dimensions a, b, c (Å), β (°)	7.7360(8), 7.3712(5), 20.856(2), 102.123(8)
a : b : c	1.050 : 1 : 2.829
Unit-cell volume (Å^3)	1162.75(19)
Z	4
Calculated density (g/cm^3)	3.052
Absorption coefficient (mm^{-1})	14.380
Crystal size (mm^3)	0.02×0.01×0.01
Data collection	
θ range	2.00 – 29.28º
h, k, l ranges	−10→ 10, −10→ 9, −28→ 28
Total reflections collected	10125
Unique reflections (R_{int})	3106 (0.198)
Unique reflections $F > 4\sigma(F)$	2677
Structure refinement	
Refinement method	Full-matrix least-squares on F^2
Weighting coefficients a, b	0.1519, 11.3786
Data/restraints/parameters	3106/0/155
R_1 [$F > 4\sigma(F)$], wR_2 [$F > 4\sigma(F)$],	0.093, 0.222
R_1 all, wR_2 all	0.102, 0.237
Goodness-of-fit on F^2	1.020
Largest diff. peak and hole, e Å^{-3}	6.057, -6.022

Table 3. Final atom coordinates and displacement parameters ($Å^2$) of atoms in the structure of beshtauite

Atom	*x*/*a*	*y*/*b*	*z*/*c*	U_{iso}
U	0.23061(5)	0.38928(6)	0.37715(2)	0.0293(3)
S1	0.5491(4)	0.7163(4)	0.45439(14)	0.0304(6)
S2	0.1430(5)	0.7270(5)	0.24760(16)	0.0356(7)
O1	0.4130(13)	0.3669(14)	0.3372(6)	0.036(2)
O2	0.0467(13)	0.4114(15)	0.4152(7)	0.040(2)
O3	0.4013(14)	0.2569(16)	0.4739(5)	0.039(2)
O4	0.3716(14)	0.6324(14)	0.4410(6)	0.038(2)
O5	0.5366(17)	0.8922(14)	0.4224(6)	0.044(3)
O6	0.6765(16)	0.5995(15)	0.4312(6)	0.043(3)
O7	0.1371(16)	0.6472(17)	0.3134(6)	0.043(2)
O8	0.0441(16)	0.2741(18)	0.2819(6)	0.049(3)
O9	0.212(2)	0.6014(18)	0.2078(8)	0.061(4)
O10	0.249(2)	0.8903(17)	0.2601(7)	0.056(3)
O_w11	0.2199(12)	0.0527(17)	0.3763(5)	0.041(3)
O_w12	0.7591(18)	0.1976(17)	0.4334(7)	0.055(3)
N1	0.6569(18)	0.7268(17)	0.2981(6)	0.040(3)
N2	0.982(2)	0.843(3)	0.4449(9)	0.060(4)

Atom	U_{11}	U_{22}	U_{33}	U_{23}	U_{13}	U_{12}
U	0.0249(3)	0.0355(4)	0.0241(3)	0.0000(1)	-0.0027(2)	-0.0008(1)
S1	0.0296(14)	0.034(2)	0.024(1)	0.001(1)	-0.0029(11)	-0.002(1)
S2	0.0349(16)	0.038(2)	0.029(1)	0.004(1)	-0.0042(12)	0.003(1)
O1	0.018(4)	0.053(6)	0.033(5)	-0.002(4)	-0.001(4)	0.013(3)
O2	0.015(4)	0.054(6)	0.048(6)	0.002(5)	-0.003(4)	0.006(4)
O3	0.039(5)	0.044(6)	0.026(4)	-0.009(4)	-0.007(4)	0.002(4)
O4	0.031(5)	0.041(6)	0.040(5)	-0.012(4)	0.006(4)	-0.014(4)
O5	0.038(6)	0.049(7)	0.041(6)	0.012(4)	-0.001(5)	-0.002(4)
O6	0.035(5)	0.051(7)	0.040(6)	-0.008(4)	0.002(5)	0.008(4)
O7	0.041(6)	0.053(6)	0.030(5)	0.012(4)	-0.002(4)	0.000(5)
O8	0.040(6)	0.061(7)	0.041(5)	-0.004(5)	-0.003(5)	-0.010(5)
O9	0.078(10)	0.059(8)	0.051(7)	0.007(5)	0.025(8)	0.026(6)
O10	0.058(8)	0.059(8)	0.045(7)	0.002(5)	0.000(6)	-0.021(5)
O_w11	0.035(5)	0.031(5)	0.045(6)	0.002(4)	-0.021(5)	0.007(4)
O_w12	0.057(7)	0.053(8)	0.059(7)	0.001(6)	0.021(6)	-0.005(6)
N1	0.051(7)	0.034(6)	0.038(6)	0.007(4)	0.018(5)	0.006(5)
N2	0.031(6)	0.094(12)	0.051(8)	0.005(8)	0.001(6)	-0.005(7)

Table 4. Selected interatomic distances (Å) in the crystal structure of beshtauite

U-O2	1.776(11)	N1···O6	2.905(17)
U-O1	1.791(10)	N1···O1	2.945(16)
U-O7	2.346(11)	N1···O10	2.921(17)
U-O8	2.355(11)	N1···O9	2.954(18)
U-O4	2.358(10)	N2···O6	2.93(2)
U-O3	2.376(10)	N2···O_w12	2.90(2)
U-O_w11	2.482(13)	N2···O_w11	2.99(2)
		N2···O_w12	3.11(2)
S1-O5	1.452(11)	S2-O9	1.419(13)
S1-O6	1.465(11)	S2-O10	1.447(12)
S1-O3	1.478(9)	S2-O8	1.490(12)
S1-O4	1.478(10)	S2-O7	1.502(11)
<S1-O>	1.468	<S2-O>	1.465

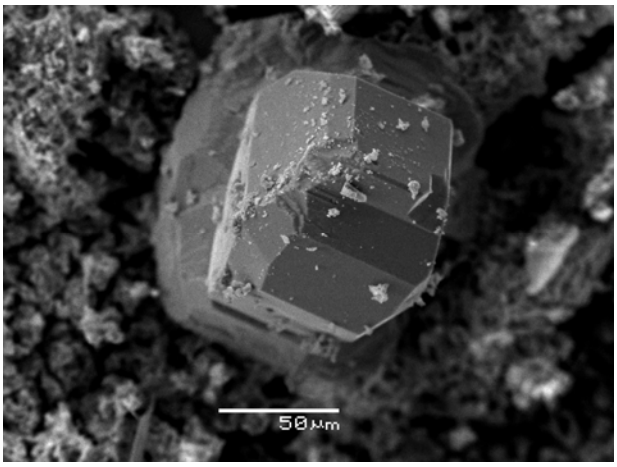

a

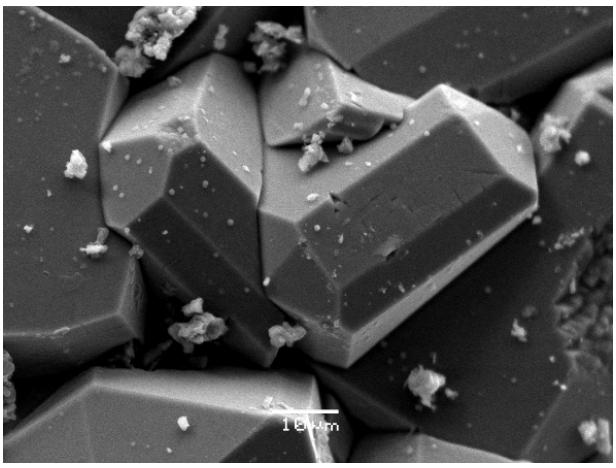

b

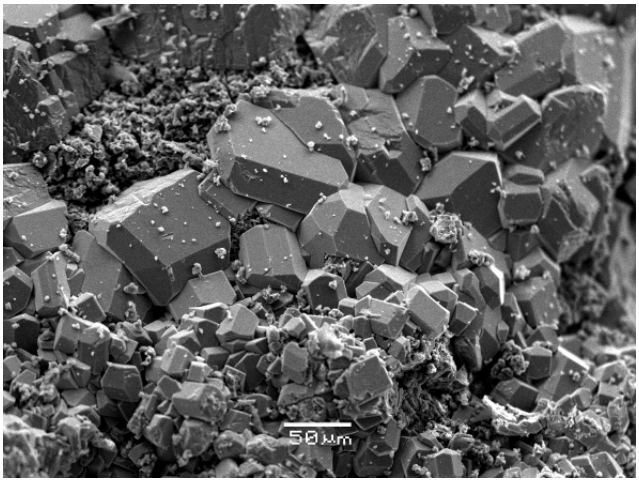

c

Figure 1. Beshtauite: typical crystal (a), crystal cluster (b) and crystal crust (c) with powdery rozenite on marcasite. SEM (SE) images.

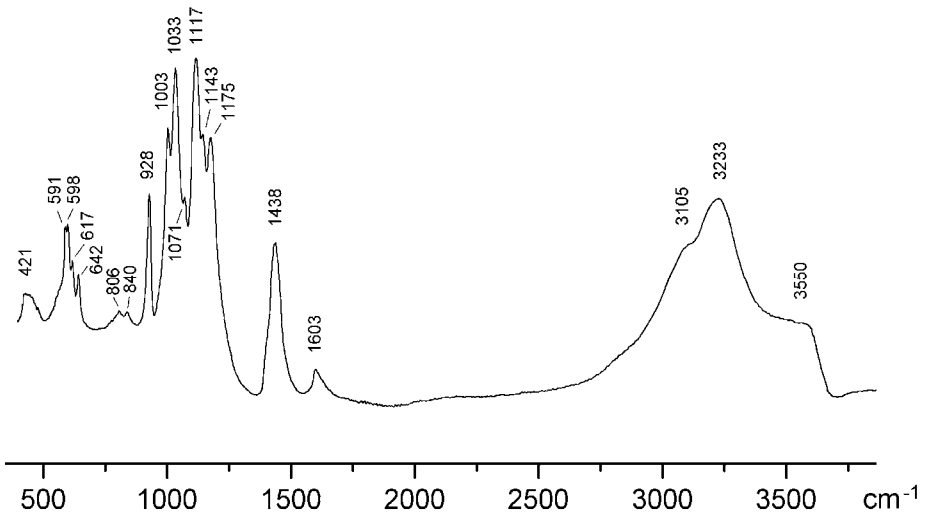

346
347 Figure 2. The IR spectrum of beshtauite.
348

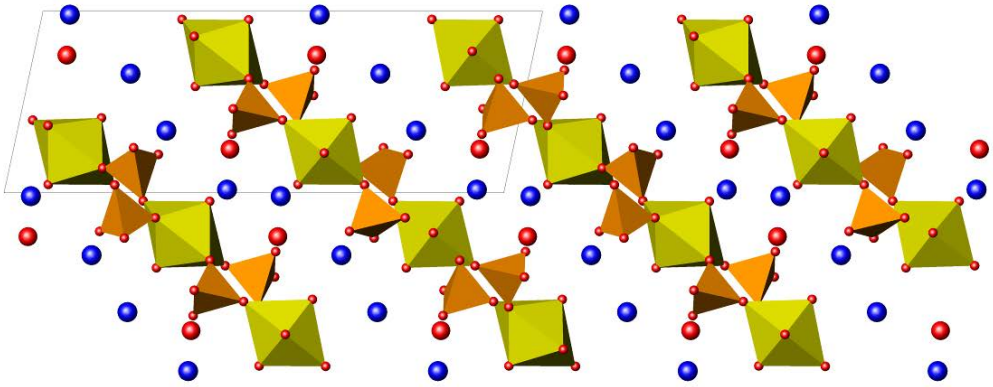

a

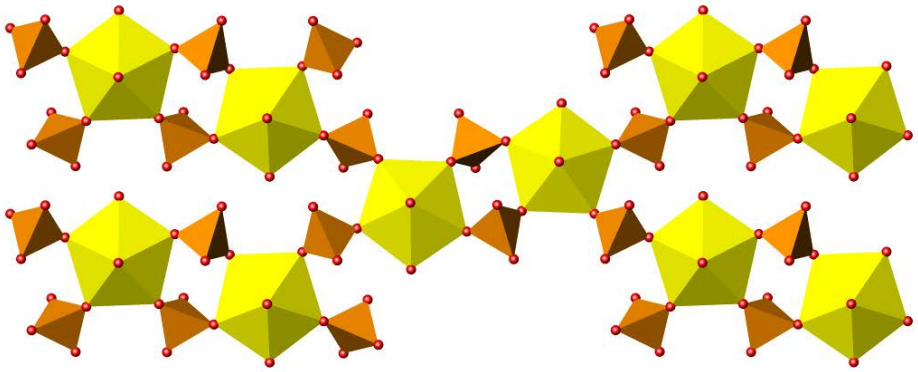

b

Figure 3. The crystal structure of beshtauite projected along the *b* axis (***a***; unit cell is outlined) and projection of the uranyl sulphate layer upon the (-102) plane (***b***). $UO_6(H_2O)$ and SO_4 groups are shown as polyhedra; O atoms of the H_2O molecules and N atoms of the ammonium cations are marked.

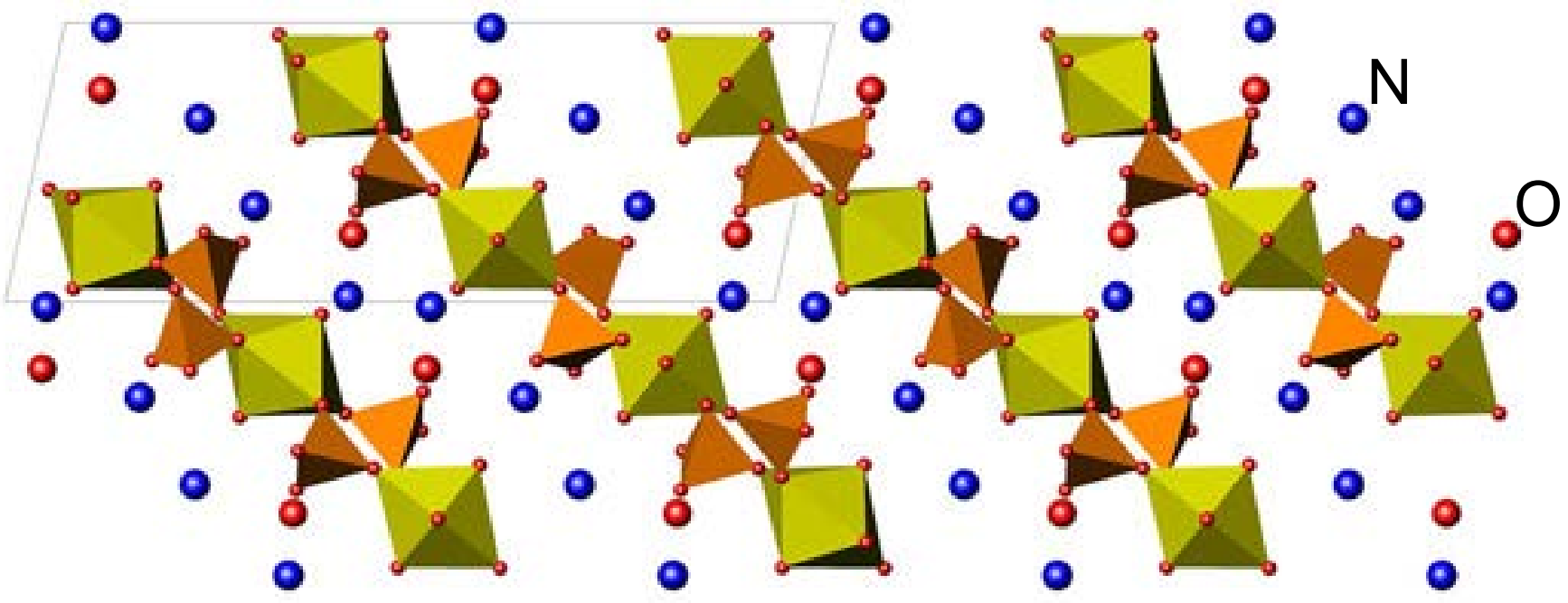
N
O

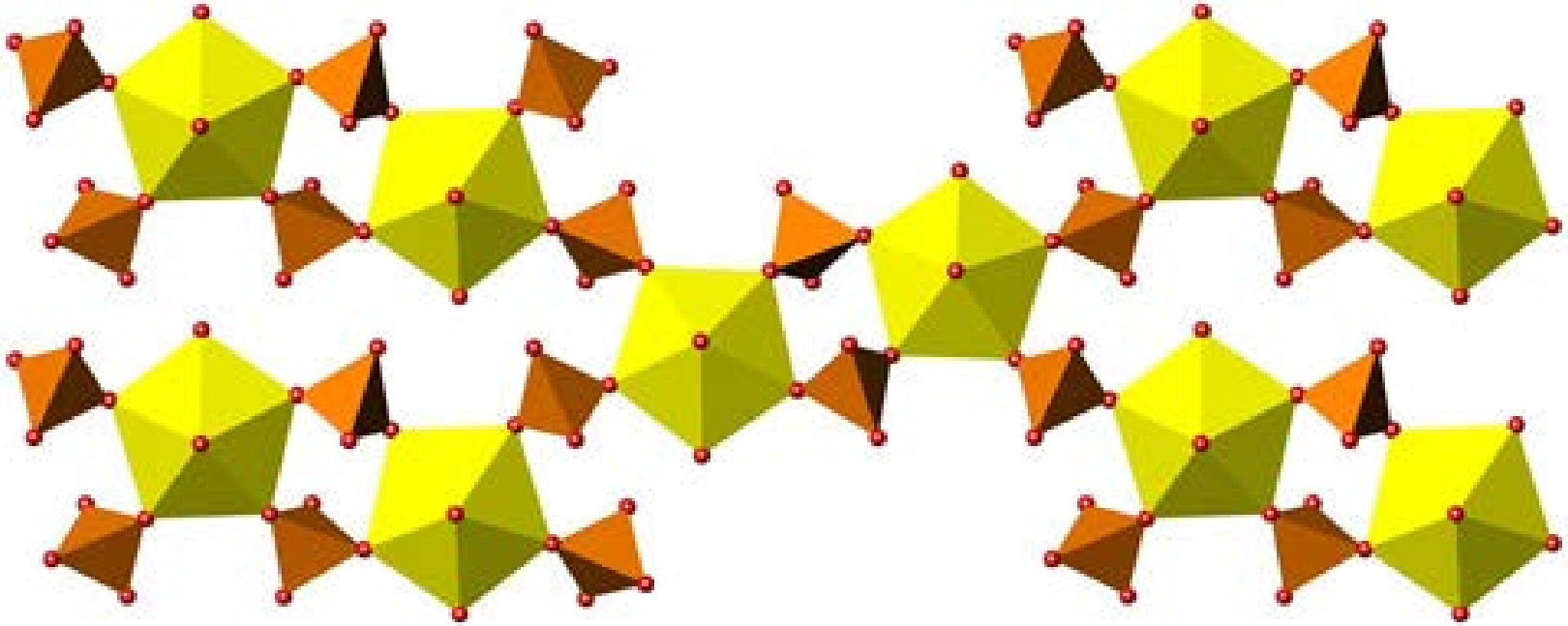

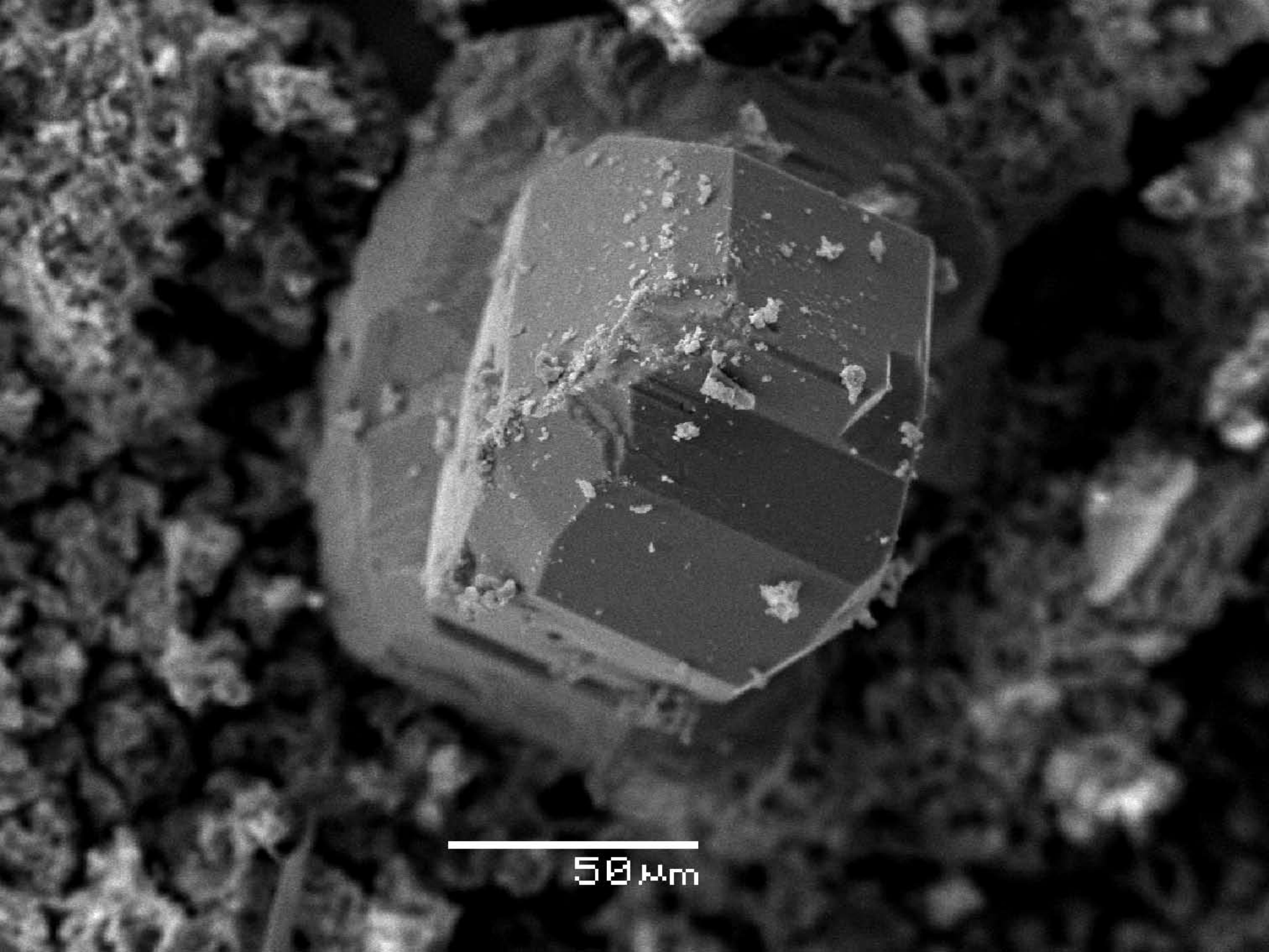
50 µm

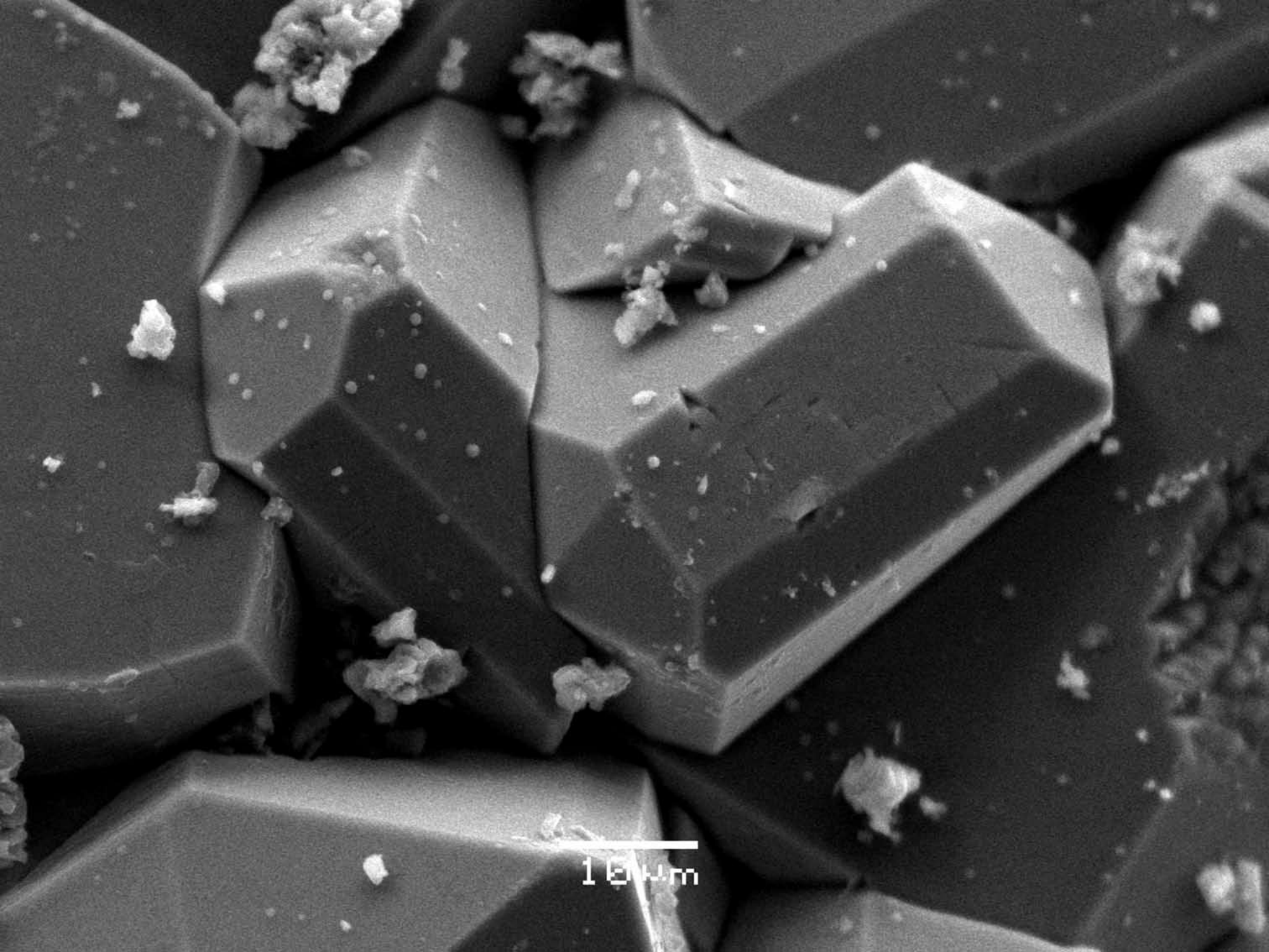
10 µm

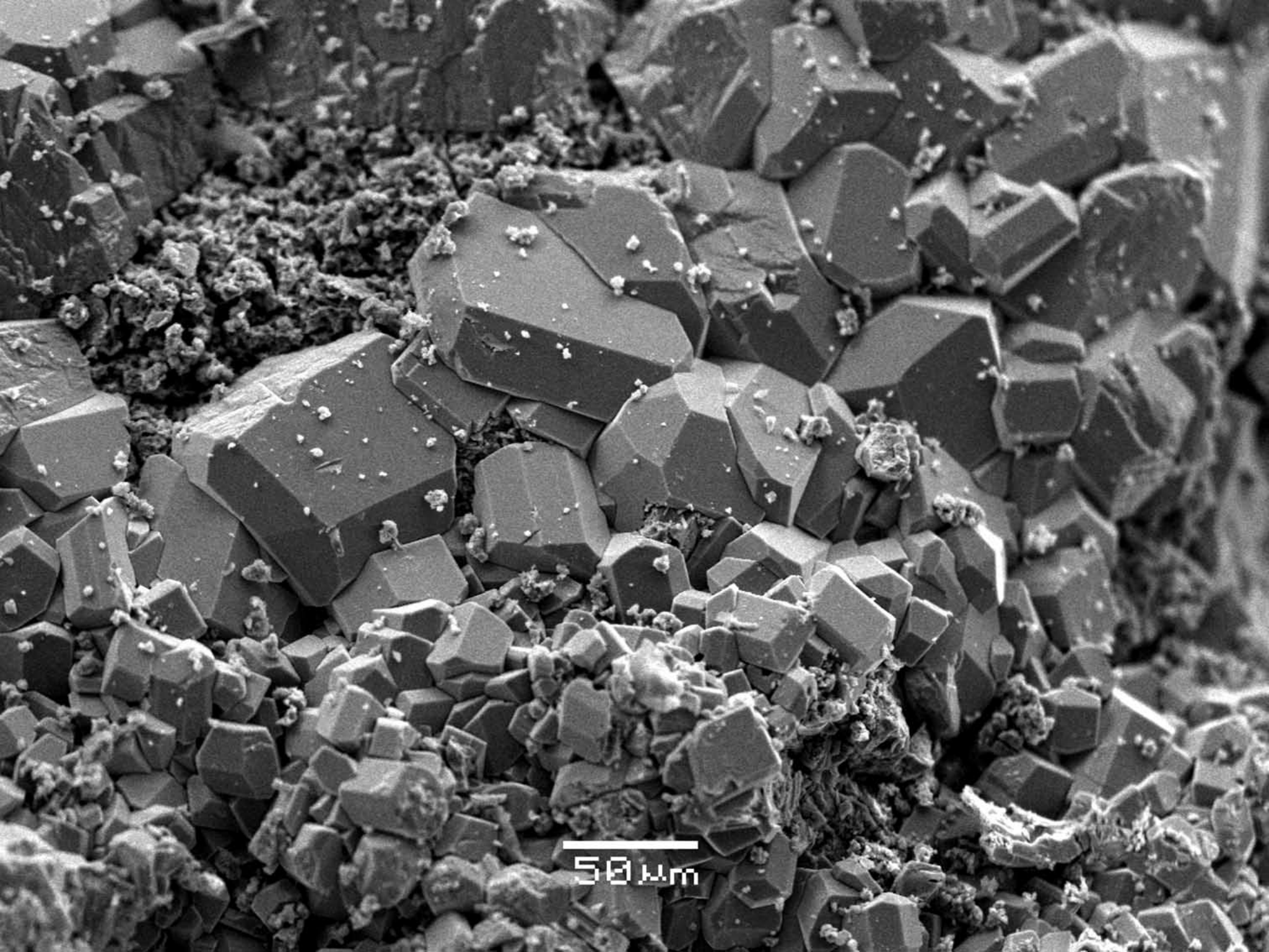
50 µm

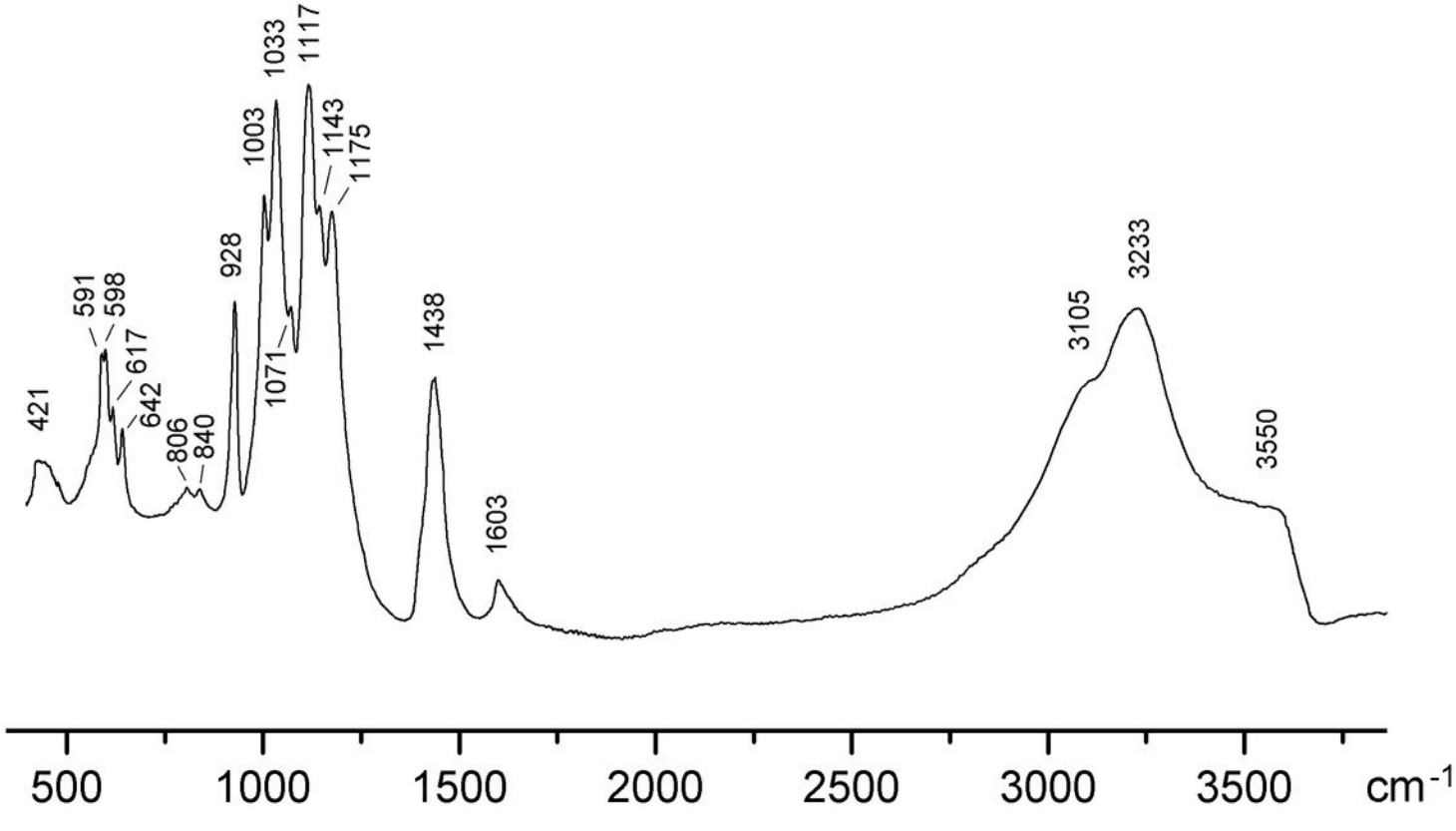
421
591
598
617
642
806
840
928
1003
1033
1071
1117
1143
1175
1438
1603
3105
3233
3550
500
1000
1500
2000
2500
3000
3500
cm-1